Available online at www.sciencedirect.com
SCIENCE DIRECT®
ELSEVIER
Physics Letters B 556 (2003) 27–32
PHYSICS LETTERS B
www.elsevier.com/locate/npe

Study of resonance states in ^{12}N using a radioactive ion beam of ^{11}C

T. Teranishi [a], S. Kubono [a], S. Shimoura [a], M. Notani [a], Y. Yanagisawa [b], S. Michimasa [a], K. Ue [a,1], H. Iwasaki [a], M. Kurokawa [a], Y. Satou [a,2], T. Morikawa [c], A. Saito [d], H. Baba [d], J.H. Lee [e], C.S. Lee [e], Zs. Fülöp [f], S. Kato [g]

[a] *Center for Nuclear Study (CNS), University of Tokyo, RIKEN campus, 2-1 Hirosawa, Wako, Saitama 351-0198, Japan*
[b] *The Institute of Physical and Chemical Research (RIKEN), 2-1 Hirosawa, Wako, Saitama 351-0198, Japan*
[c] *Department of Physics, Kyushu University, 6-10-1 Hakozaki, Fukuoka 812-8581, Japan*
[d] *Department of Physics, Rikkyo University, Toshima, Tokyo 171-8501, Japan*
[e] *Department of Physics, Chun-Ang University, Seoul 156-756, South Korea*
[f] *Institute of Nuclear Research (ATOMKI), PO Box 51, H-4001 Debrecen, Hungary*
[g] *Department of Physics, Yamagata University, Yamagata 990-8560, Japan*

Received 5 August 2002; received in revised form 15 January 2003; accepted 20 January 2003

Editor: J.P. Schiffer

Abstract

Resonance states in ^{12}N were studied by using the resonance elastic scattering of $^{11}\mathrm{C} + \mathrm{p}$ with a low-energy radioactive ion beam of ^{11}C at 3.5 MeV/nucleon and a thick $(\mathrm{CH}_2)_n$ target. The ^{11}C beam was separated by a newly installed CNS radioactive ion beam separator (CRIB). The energy spectrum of recoil protons was measured at laboratory scattering angles around $\theta_{\mathrm{LAB}} = 0°$ to identify resonance states in ^{12}N. The spin-parity values of $J^\pi = 3^-$ and $(2)^+$ have been determined for the levels at the excitation energies of $E_x = 3.1$ and 3.6 MeV in ^{12}N, respectively, suggesting a small contribution of the 3.1-MeV level to the $^{11}\mathrm{C}(\mathrm{p},\gamma)^{12}\mathrm{N}$ stellar reaction.

PACS: 21.10.Hw; 25.40.Ny; 26.20.+k; 27.20.+n

Keywords: Resonance states; Elastic scattering; Radioactive ion beam; Nuclear astrophysics

Experimental studies on unstable nuclei using low-energy radioactive ion (RI) beams are very useful to investigate low-energy nuclear properties, especially, for astrophysical interests. We have developed an extensive low-energy RI beam separator of in-flight type for this purpose. The choice of in-flight type, instead of ISOL, allows us to produce RI beams rather easily due to its technical simplicity in extracting RI from targets. On the other hand, ISOL type separators often require elaborate works on ion sources, whose

E-mail address: teranisi@cns.s.u-tokyo.ac.jp (T. Teranishi).
[1] Present address: Department of Physics, University of Tokyo, 7-3-1 Hongo, Bunkyo-ku, Tokyo 113-0033, Japan.
[2] Present address: Department of Physics, Tokyo Institute of Technology, 2-12-1, Oh-okayama, Meguro, Tokyo 152-8551, Japan.

0370-2693/03/$ – see front matter
doi:10.1016/S0370-2693(03)00098-4

efficiencies depend on the chemical properties of RI to be extracted. Using the low-energy in-flight separator, we have performed the first experiment of the elastic resonance scattering of $^{11}C + p$ to study resonance states in ^{12}N.

Resonance states just above the proton threshold in ^{12}N have been discussed in conjunction with the astrophysical reaction rate of $^{11}C(p,\gamma)^{12}N$ [1–4]. This reaction could play a key role for production of heavy elements of $A \geqslant 12$ from light elements of the primordial origin [5]. This reaction would have a large influence on the fate of metal-deficient massive stars, which can be classified as Population III, in the early universe. Although the stellar reaction rate of $^{11}C(p,\gamma)^{12}N$ cannot be determined from the data of $^{11}C + p$ elastic scattering, it is important to know precisely the energies, total widths, and spin-parities (J^π) of the levels as well as to search for new levels above the proton threshold. The low-lying levels in ^{12}N were previously studied mainly by the $^{10}B(^3He,n)^{12}N$ and $^{12}C(^3He,t)^{12}N$ reactions [6]. However, as discussed later, some of the levels are not well known in terms of J^π. The present experiment of $^{11}C + p$ gives an alternative way to investigate the ^{12}N levels.

In the present Letter, we observed the elastic resonance scattering of $^{11}C + p$ in inverse kinematics, $p(^{11}C,p)$. A low-energy ^{11}C beam was used in the thick target method [7–9]. In this method, the energies of recoil protons, coming out from a thick target, are measured at a forward angle in the laboratory frame and then converted to the center-of-mass energies of scattering. Due to the thick target, a wide range of the excitation function for the elastic scattering can be measured with a beam of fixed energy. A resonance state, if it exists with a sufficiently large width, can be identified in the excitation function as an interference pattern of potential and resonance scattering. The resonance energy, width, and J^π can be determined from the excitation function. Therefore, this method is very useful to study proton resonances in proton-rich unstable nuclei [10–13]. In this Letter, we report the first experimental result on the elastic resonance scattering of $^{11}C + p$ using the RI beam of ^{11}C. Some J^π assignments have been made successfully for the low-lying levels in ^{12}N above the proton threshold.

The experiment was performed using the CNS radioactive ion beam separator (CRIB) [14], which was recently installed by CNS, in the RIKEN accelerator research facility. Fig. 1 shows the experimental setup. A primary beam of ^{10}B was accelerated up to 7.8 MeV/nucleon by an AVF cyclotron with $K = 70$. The primary beam bombarded a ^3He gas target with a thickness of 0.25 mg/cm^2. The target gas was confined in a small chamber with entrance and exit windows. The gas pressure was 1 atmosphere and Havar foils of 2.2-μm thick were used for the windows. A secondary beam of ^{11}C was produced by the $^3He(^{10}B, {}^{12}N^*)n$ reaction, where the ^{11}C particles were emitted from the unbound levels in ^{12}N. The secondary ^{11}C particles were separated by CRIB, which consisted of two dipole and four quadrupole magnets.

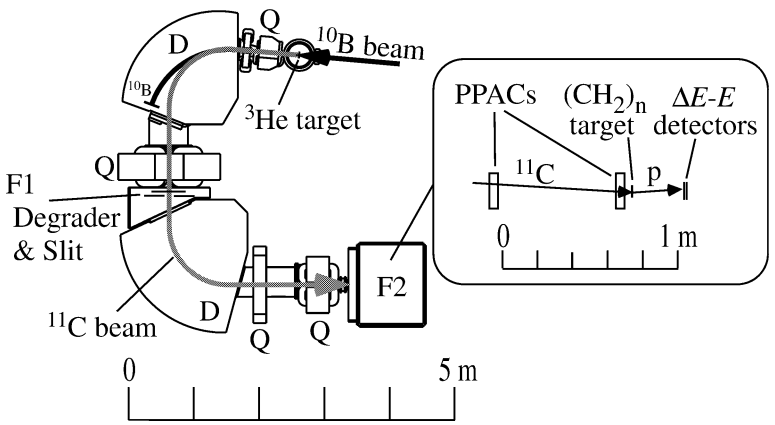

Fig. 1. Setup for the production of the ^{11}C beam using the separator CRIB. The experimental setup for the $^{11}C + p$ scattering was installed in the chamber at F2.

The primary beam of ^{10}B was removed from the secondary beam by the first dipole magnet and stopped by a beam dump on an inner wall of the magnet. There were two focal planes, a momentum dispersive focal plane (F1) between the two dipole magnets and an achromatic focal plane (F2) at the end of the separator. An energy degrader of 10-μm thick Mylar foil was installed at F1 to remove background light ions from the secondary beam. A horizontal slit was set at F1 to select the ^{11}C particles in an energy region of 4.5–4.7 MeV/nucleon after the degrader.

At F2, a setup for the $^{11}\mathrm{C} + \mathrm{p}$ scattering was installed inside a vacuum chamber (the inset in Fig. 1). The setup consisted of two parallel-plate avalanche counters (PPACs) [15], a $(\mathrm{CH}_2)_n$ target with a thickness of 8.0 mg/cm^2, and a pair of ΔE–E silicon detectors with thicknesses of 70 and 1500 μm, respectively. Each PPAC was capable of measuring timing and two-dimensional hit position. The identification of ^{11}C was made event-by-event by using time-of-flight between the two PPACs. The beam profile on the target was also monitored by the position information of the PPACs. The beam intensity of ^{11}C was 1.7×10^4 particles/s, which was about 17% of the total secondary-beam intensity. The major contaminant in the beam was ^{10}B caused by scattering of the primary beam at inner walls of the magnets. The beam spot widths were 18 mm (FWHM) horizontally and 13 mm (FWHM) vertically. The horizontal and vertical angular widths of the beam were 25 mrad (FWHM) and 53 mrad (FWHM), respectively. The energy of the ^{11}C beam after the PPACs was 3.5 MeV/nucleon with a width of 0.2 MeV/nucleon (FWHM).

The ^{11}C particles were fully stopped in the $(\mathrm{CH}_2)_n$ target and the recoil protons, which went out from the target, were detected by the ΔE and E detectors. The ΔE and E detectors were mounted at 30-cm downstream of the target and were centered at the laboratory angle $\theta_{\mathrm{LAB}} = 0°$ (the center-of-mass angle $\theta_{\mathrm{CM}} = 180°$), covering $\theta_{\mathrm{LAB}} = 0°$–$5°$ ($\theta_{\mathrm{CM}} = 170°$–$180°$). The ΔE detector had double-sided strips, which were used to determine the two-dimensional hit position. By the proton hit position and the PPAC angular information, the scattering angle was determined with a resolution of $\Delta\theta_{\mathrm{LAB}} = 0.6°$ (FWHM). The identification of proton was made by using the ΔE–E information and time-of-flight measured by the PPACs and the ΔE detector. From the sum of the energies measured by the ΔE and E detectors, the proton energy (E_{p}) after the target was deduced with a resolution of 170 keV (FWHM). The calibration of E_{p} was performed by using secondary proton beams separated by CRIB at several energy points.

One can convert E_{p} to the center-of-mass energy (E_{CM}) by taking into account the kinematics of $^{11}\mathrm{C} + \mathrm{p}$ and energy loss of particles in the target. The resolution of E_{CM} was deduced to be 50 keV (FWHM) from the E_{p} resolution, the θ_{LAB} resolution, the beam energy width, and energy straggling of particles in the target. This resolution is much better than the E_{p} resolution because of the kinematic factor of $dE_{\mathrm{CM}}/dE_{\mathrm{p}} \sim 0.3$ at $\theta_{\mathrm{LAB}} \sim 0°$. The systematic error in deducing E_{CM} was estimated to be ± 20 keV, which came mainly from those of E_{p} and the beam energy. Since the proton threshold in ^{12}N is 0.601 MeV [6], the excitation energy in ^{12}N is $E_x = E_{\mathrm{CM}} + 0.601$ MeV.

A data with a C target (10.7 mg/cm^2) was also taken in a separate run to evaluate the background contribution from the reactions of ^{11}C with C atoms in the $(\mathrm{CH}_2)_n$ target. The proton spectrum with the C target had a bump shape centered at $E_{\mathrm{p}} \sim 6$ MeV with a width of ~ 4 MeV (FWHM) and without any sharp structure. The yield normalization for the two proton spectra with the $(\mathrm{CH}_2)_n$ and C targets was made by number of beam particles and by target thickness per unit energy loss of beam. After the normalization, the proton yield in the spectrum with the C target was about 1/5 of that with the $(\mathrm{CH}_2)_n$ target. Then, the spectrum for the H target was deduced by subtracting the normalized spectrum with the C target from that with the $(\mathrm{CH}_2)_n$ target. Finally, the vertical scale of the spectrum was converted from counts to $d\sigma/d\Omega$ by using the energy-dependent target thickness inversely proportional to the beam stopping power (see Eq. (9) in Ref. [9]), the detector solid angle, and the total beam particles of 3.14×10^9 for the spectrum.

Fig. 2 shows the experimental result of the proton spectrum for the $^{11}\mathrm{C} + \mathrm{p}$ scattering. The spectrum covers a region of $E_{\mathrm{CM}} = 0.3$–3.1 MeV. The error bars indicate the statistical errors only. The systematic error in the absolute magnitude of $d\sigma/d\Omega$ is $\pm 4\%$, which is mainly due to that in the detector solid angle. The events in $E_{\mathrm{p}} = 2.3$–2.7 MeV ($E_{\mathrm{CM}} = 0.73$–0.85 MeV) were not always registered with correct energies due to the dead layers between the ΔE and E silicon detectors. These events were

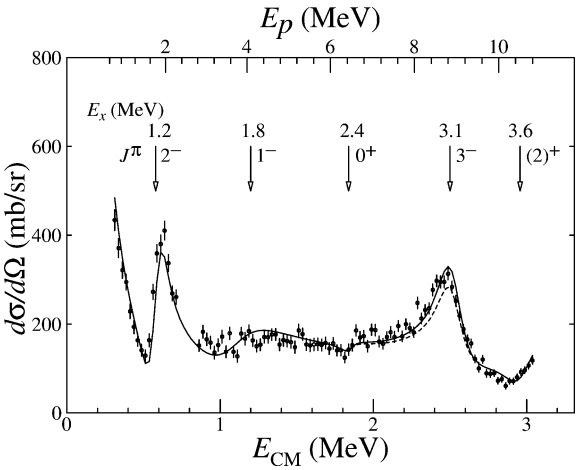

Fig. 2. Experimental proton spectrum for the $^{11}C + p$ elastic scattering. The vertical scale is the $d\sigma/d\Omega$ averaged over the detector solid angle ($\sim d\sigma/d\Omega$ at $\theta_{CM} = 180°$). The solid line is a result by the resonance formula with the parameters in Table 2. The dashed line represents the spectral shape for $J^\pi = 2^-$ at $E_x = 3.1$ MeV. Arrows indicate resonance energies. A rough scale of proton energy (E_p) is also displayed.

Table 1
Levels in ^{12}N above the proton threshold. The present experimental spectrum is consistent with the E_x and Γ values for the levels at $E_x = 1.2$–3.6 MeV and the J^π values for the levels at $E_x = 1.2$–2.4 MeV

J^π	E_x (MeV)	Γ (MeV)	$J^{\pi\,c}$
$2^{+\,a}$	0.960 ± 0.012^a	$< 0.020^a$	
$2^{-\,a}$	1.191 ± 0.008^a	0.118 ± 0.014^a	
$1^{-\,a}$	1.80 ± 0.03^a	0.75 ± 0.25^a	
$0^{+\,a}$	2.439 ± 0.009^a	0.068 ± 0.021^a	
$2^+, 3^{-\,a}, (3^-)^b$	3.132 ± 0.008^a	0.220 ± 0.020^a	3^-
$(1)^{+\,a}, (1^-, 2^+)^b$	3.558 ± 0.009^a	0.220 ± 0.025^a	$(2)^+$
$2^{-\,b}$	4.18 ± 0.05^b	0.836 ± 0.025^b	
$4^{-\,b}$	4.41 ± 0.05^b	0.744 ± 0.025^b	

[a] From Ref. [6].
[b] From Ref. [21].
[c] Present work.

removed from the spectrum. There are six known ^{12}N levels in the spectral range ($E_x = 0.9$–3.7 MeV) as listed in Table 1. The spectrum clearly shows an interference pattern of potential scattering and resonance scattering. Two peaks are prominently seen at $E_{CM} \sim 0.6$ and ~ 2.5 MeV. These are due to the resonance states at $E_x = 1.2$ and 3.1 MeV, respectively. No clear signature of the first 2^+ level at $E_x = 0.96$ MeV ($E_{CM} \sim 0.36$ MeV) is seen in the spectrum because its width is too narrow ($\Gamma < 20$ keV and probably $\Gamma \sim 5.5$ keV [3]) compared with the energy resolution. A flat distribution of events at $E_{CM} = 1.0$–1.7 MeV is due to the wide ($\Gamma = 0.75$ MeV) level of 1^- at $E_x = 1.8$ MeV. A contribution from the narrow ($\Gamma = 0.068$ MeV) level of 0^+ at $E_x = 2.4$ MeV can be seen as a small dip at $E_{CM} \sim 1.8$ MeV. A valley of yield at $E_{CM} \sim 2.9$ MeV is due to the level at $E_x = 3.6$ MeV. An increase of yield with energy at $E_{CM} > 2.9$ MeV can be explained partly by contributions from the levels at $E_x = 4.2$ and 4.4 MeV, which are out of the spectral range.

A calculation utilizing a resonance formula was performed to derive $d\sigma/d\Omega$ and the result was compared with the experimental spectrum. The formula is based on Ref. [16] and involves potential scattering (Rutherford + hard-sphere) amplitudes and a sum of single-level resonance amplitudes for the seven levels from $E_x = 1.2$ to 4.4 MeV. For the sake of simplicity, we assume that only a single-particle proton orbit of ℓ_j contributes to a resonance. This may be a good approximation for the low-lying negative-parity levels ($2s_{1/2} \otimes 1p_{3/2}^{-1}$ or $1d_{5/2} \otimes 1p_{3/2}^{-1}$) with $T = 1$ in $A = 12$ nuclei [17–20]. The level width Γ_R is defined as $\Gamma_\ell(E_R)$, where E_R is the resonance energy and Γ_ℓ is the energy-dependent proton width proportional to the penetration factor for ℓ. Since the channel spin can be $s = 1$ or 2 for the spin pair of $I_1 = 3/2$ (^{11}C) and $I_2 = 1/2$ (proton), Γ_ℓ is equal to the sum of the partial widths for the two s values ($\Gamma_\ell = \sum_s \Gamma_{s\ell}$). A single-level resonance amplitude for the $s \to s'$ scattering is proportional to $i g_{s\ell} g_{s'\ell}/(E_R + \Delta_\ell - E_{CM} - i\Gamma_\ell/2)$, where $g_{s\ell} = \pm\Gamma_{s\ell}^{1/2}$ as defined in Ref. [16] and Δ_ℓ is the energy shift with the boundary condition of $\Delta_\ell(E_R) = 0$. Due to the pure ℓ_j orbit, $g_{s\ell}$ may be proportional to the Racah recoupling-transformation coefficient between the two coupling schemes of ($\vec{I}_1 + \vec{I}_2 = \vec{s}$; $\vec{s} + \vec{\ell} = \vec{J}$) and ($\vec{\ell} + \vec{I}_2 = \vec{j}$; $\vec{I}_1 + \vec{j} = \vec{J}$). The $g_{s\ell}$ value was deduced from this coefficient and the input parameters of E_R and Γ_R. The corrections for the finite detector solid angle and the detector energy resolution were also included in the calculation.

The solid line in Fig. 2 indicates the result of calculation with the resonance parameters shown in Table 2. A channel radius of 4.5 fm [18,19] is used for the resonances and the hard-sphere scattering. The E_R, Γ_R and J^π values were taken from Refs. [6,21]. The ℓ of the proton orbit for each level is also shown

Table 2
Resonance parameters for the proton spectrum shown by the solid line in Fig. 2

E_R (MeV)	0.59[a]	1.20[a]	1.84[a]	2.53[a]	2.96[a]	3.58[b]	3.81[b]
Γ_R (MeV)	0.12[a]	0.75[a]	0.07[a]	0.22[a]	0.22[a]	0.84[b]	0.74[b]
J^π	2^-	1^-	0^+	3^-	2^+	2^-	4^-
ℓ	0	0	1	2	1	2	2

[a] From Ref. [6].
[b] From Ref. [21].

in Table 2. For s- and d-waves, the corresponding proton orbits were assumed to be $2s_{1/2}$ and $1d_{5/2}$, respectively. For the 0^+ level, $1p_{3/2}$ is taken since $j = 3/2$ is required to make $J = |\vec{l}_1 + \vec{j}| = 0$. In the level at $E_x = 3.6$ MeV, $1p_{3/2}$ and $1p_{1/2}$ components may be comparably mixed. However, $1p_{1/2}$ was tentatively taken for this level, producing almost the same result as one taking $1p_{3/2}$. The theoretical curve agrees well with the experimental spectrum, indicating that all the known E_R and Γ_R of the levels at $E_x = 1.2$–3.6 MeV are consistent with the present spectrum. The simplification of no ℓ-mixing in each level seems to be also supported by the agreement of the spectral shape.

The J^π of the level at $E_x = 3.1$ MeV was previously assigned to be 2^+ or 3^- [6]. The data of the ^{12}C(p, n)^{12}N reaction [21], which was measured after the level compilation of Ref. [6], gave an assignment of $J^\pi = (3^-)$. Our experimental result is consistent with the calculation with $J^\pi = 3^-$ (d-wave) for this level. A result taking $J^\pi = 2^+$ (p-wave) and keeping the same width does not reproduce the peak at $E_{\mathrm{CM}} \sim 2.5$ MeV, and gives, instead, a valley of yield there. Therefore, the possibility of 2^+ at this energy is excluded. The peak height depends on the J value and is consistent with $J^\pi = 3^-$. Taking a different possible J value (0, 1, 2, or 4) for the d-wave resonance gives a worse fit to the experimental peak. For example, the peak for $J^\pi = 2^-$, shown by the dashed line in Fig. 2, has a lower height than the 3^- peak height by 14%, while the uncertainty in the calculated peak height is only ± 2 % due to the uncertainty in the E_R and Γ_R parameters. The peak height may also change if an s-wave component is largely admixed in this level. Such a mixture, possible only for $J^\pi = 1^-$ and 2^-, modifies also the peak shape considerably and makes the fit further worse. The present assumption of the pure $d_{5/2}$ orbit for the d-wave resonance can be justified by indications of small $d_{3/2}$ contributions to low-lying $T = 1$ levels in $A = 12$ nuclei [17–20]. From the above considerations, we adopt $J^\pi = 3^-$ here for the 3.1-MeV level.

The J^π of the level at $E_x = 3.6$ MeV was previously assigned to be $(1)^+$ in Ref. [6] and $(1^-,\ 2^+)$ in Ref. [21]. A result of the present calculation taking $J^\pi = 1^-$ (s- or d-wave) produces a peak at $E_{\mathrm{CM}} \sim 2.9$ MeV, and therefore, is not consistent with the experimental spectrum. On the other hand, both results taking $J^\pi = 2^+$ (p-wave), as shown by the solid line in Fig. 2, and 1^+ (p-wave) reproduce the valley of yield there. However, it is difficult to determine uniquely the J value from the depth of the valley because the contributions from higher levels are not taken into account precisely. If we compare the $T = 1$ triplets in $A = 12$ nuclei (see Fig. 2 in Ref. [21]), $J^\pi = 2^+$ is more likely for this level, because there is no 1^+ ($T = 1$) level near the first 3^- ($T = 1$) level in ^{12}B (^{12}C). Therefore, we tentatively adopt $J^\pi = (2)^+$ for the 3.6-MeV level.

The inelastic scattering p(^{11}C, ^{11}C*)p could occur at the energies above $E_{\mathrm{CM}} = 2.0$ MeV since the first excited state in ^{11}C is at $E_x = 2.0$ MeV [6]. In the present experimental condition, recoil protons by the inelastic scattering should have $E_{\mathrm{p}} = 1.7$–7.4 MeV when they come out from the target. There is no significant excess of events in this region of the experimental spectrum as compared with the theoretical curve. Therefore, the contribution of the inelastic scattering to the spectrum is considered to be negligible.

In the stellar reaction of ^{11}C(p, γ)^{12}N, the lowest three excited levels in ^{12}N at $E_x = 0.96$, 1.2, and 1.8 MeV were suggested to play important roles at the temperature region of $T_9 < 1$ [1]. The energies and widths for the latter two levels have been confirmed by the present experiment. The assignment of $J^\pi = 3^-$ has been made for the level at $E_x = 3.1$ MeV. Therefore, we can conclude that the 3.1-MeV level does not contribute to the (p, γ) reaction rate so

much, even at $T_9 > 1$, since the level decays by M2 or E3 transitions to the ^{12}N (g.s.; 1^+), which is the unique bound state in ^{12}N. The (p,γ) reaction rate was investigated experimentally by the Coulomb dissociation of ^{12}N [3,4]. However, the most crucial resonance parameters, the gamma widths, have been determined only for the 1.2-MeV level with a large uncertainty. Thus, the reaction rate is still an open question and the gamma width measurements are the next experimental goal for the present stellar reaction.

In summary, we observed the elastic resonance scattering of $^{11}\mathrm{C} + \mathrm{p}$ using an RI beam of ^{11}C, obtained from the newly installed RI beam separator CRIB. In the recoil proton spectrum, levels in ^{12}N were identified in the region of $E_x = 0.9$–3.7 MeV. We have made the assignments of $J^\pi = 3^-$ and $(2)^+$ for the levels at $E_x = 3.1$ and 3.6 MeV, respectively. The present new J^π assignment suggests a small contribution of the 3.1-MeV level to the $^{11}\mathrm{C}(\mathrm{p},\gamma)^{12}\mathrm{N}$ stellar reaction. The present results of $^{11}\mathrm{C} + \mathrm{p}$ clearly demonstrate a capability of the present experimental technique, the low-energy RI beam separator of in-flight type for nuclear spectroscopy on unstable nuclei.

Acknowledgements

We would like to thank Dr. S. Watanabe, Mr. Y. Ohshiro, Mr. N. Yamazaki, and Dr. Y. Mizoi for their contribution to the construction of CRIB. We also thank the CNS/RIKEN staff members for their operation of the ion source and the cyclotron. We are grateful to Prof. T. Motobayashi and Mr. T. Minemura for their experimental information. The present study was partially supported by Grant-in-Aid for Science Research from the Japan Ministry of Education, Culture, Sports, and Technology under the contract numbers 13440071 and 14740156, and also by the Joint Research Program under the Korea–Japan Basic Science Promotion Program (KOSEF 2002-JR015).

References

[1] M. Wiescher, et al., Astrophys. J. 343 (1989) 352.
[2] P. Descouvemont, et al., Nucl. Phys. A 646 (1999) 261.
[3] A. Lefebvre, et al., Nucl. Phys. A 592 (1995) 69.
[4] T. Minemura, et al., RIKEN Accel. Prog. Rep. 35 (2002) 58; T. Minemura, et al., private communication.
[5] R. Mitalas, Astrophys. J. 290 (1985) 273.
[6] F. Ajzenberg-Selove, Nucl. Phys. A 506 (1990) 1.
[7] K.P. Artemov, et al., Sov. J. Nucl. Phys. 52 (1990) 408.
[8] A. Huerta Hernández, et al., Nucl. Instrum. Methods B 143 (1998) 569.
[9] S. Kubono, Nucl. Phys. A 693 (2001) 221.
[10] R. Coszach, et al., Phys. Rev. C 50 (1994) 1695.
[11] K. Markenroth, et al., Phys. Rev. C 62 (2000) 034308.
[12] A. Galindo-Uribarri, et al., Nucl. Instrum. Methods B 172 (2000) 647.
[13] C. Ruiz, et al., Phys. Rev. C 65 (2002) 042801.
[14] S. Kubono, et al., Eur. Phys. J. A 13 (2002) 217; Y. Yanagisawa, et al., RIKEN Accel. Prog. Rep. 34 (2001) 183.
[15] H. Kumagai, et al., Nucl. Instrum. Methods A 470 (2001) 562.
[16] J.M. Blatt, L.C. Biedenharn, Rev. Mod. Phys. 24 (1952) 258.
[17] V. Gillet, N.V. Mau, Nucl. Phys. 54 (1964) 321.
[18] R.O. Lane, et al., Phys. Rev. C 2 (1970) 2097.
[19] P.E. Koehler, et al., Nucl. Phys. A 394 (1983) 221.
[20] S.S. Hanna, et al., Phys. Rev. C 25 (1982) 1179.
[21] B.D. Anderson, et al., Phys. Rev. C 54 (1996) 237.